EPJ Web of Conferences **334**, 04007 (2025) https://doi.org/10.1051/epjconf/202533404007
TGF'24

Gait synchronisation in pedestrian dyads: the influence of social interaction

Adrien GREGORJ[1], *Zeynep* YÜCEL[1,2,3,*], *Francesco* ZANLUNGO[2,4,5], and *Takayuki* KANDA[2,6]

[1]Okayama University, Okayama, Japan
[2]ATR International, Kyoto, Japan
[3]Ca' Foscari University of Venice, Venice, Italy
[4]Osaka International Professional University, Osaka, Japan
[5]University of Palermo, Palermo, Italy
[6]Kyoto University, Kyoto, Japan

Abstract. Spontaneous gait synchronisation is commonly observed in pedestrian groups and has been studied extensively in controlled settings. Here, we investigate this phenomenon in a natural environment using a pedestrian trajectory dataset collected with range sensors in a public space, along with annotations for social groups and their interaction levels. To quantify synchronisation, we analyze the lateral periodic swaying of pedestrians, computed as orthogonal displacements from smoothed trajectories. Using the Hilbert transform, we derive instantaneous phase of pedestrians' gait residuals and then compute relative phases for all dyads. Additionally, we calculate the Gait Synchronisation Index (GSI) to quantify the level of synchronisation between pedestrians. Results show significantly higher GSI, stronger phase locking around zero, and lower phase variance in dyads with high interaction levels compared to less interactive pairs and randomly chosen pairs of pedestrians. These findings highlight the role of social interaction in gait synchronisation and provide insights into crowd dynamics and motor coordination, with potential applications in socially-aware robotics and intelligent transportation systems.

1 Introduction and Objectives

Spontaneous gait synchronisation is a phenomenon commonly observed in pedestrian groups, where individuals naturally adjust their gait to align with one another. This behavior has been studied extensively in controlled experimental settings [1], and has been linked to a variety of factors such as biomechanical properties [2], sensory feedback [3], or cognitive demands [4]. However, studies based on ecological data, such as pedestrian trajectories collected in natural environments, remain relatively scarce [5], and even these data based on curated online videos may be subject to a selection bias [6].

In this study, we investigate spontaneous gait synchronisation in social groups in a natural environment, using a pedestrian trajectory dataset collected via range sensors in a public space. The dataset includes annotations identifying social groups and the levels of interaction

*e-mail: zeynep@atr.jp

between group members, allowing us to explore the relationship between social dynamics and gait synchronisation.

To analyze synchronisation, we compute the lateral periodic swaying of pedestrians, referred to as gait residuals, by measuring orthogonal displacements from smoothed trajectories. The Hilbert transform is then applied to these residuals to extract the instantaneous phase of each pedestrian's motion. From these, the relative phase for each pair of pedestrians is computed as the difference between their respective phases. The phase locking and its variance are used to evaluate synchronisation stability. Additionally, we calculate the Gait Synchronisation Index [7], which quantifies synchronisation based on the entropy of the relative phase distribution, with values ranging from 0 (no synchronisation) to 1 (perfect synchronisation).

Our analysis focuses on dyads (two-person groups) to explore the influence of social interactions on gait synchronisation. The results reveal that dyads with higher interaction levels demonstrate significantly greater GSI, more pronounced phase locking near zero, and reduced phase variance compared to less interactive pairs and randomly chosen pairs of pedestrians.

This study of natural pedestrian behavior improves our understanding of the complex interplay between social factors and gait synchronisation adding on previous works on proxemics and entrainment [8–11]. The findings provide important insights into crowd dynamics and hold potential applications in socially-aware robotics, intelligent transportation systems, and the design of public spaces.

2 Related Work

Metrics for quantifying gait synchronisation have evolved significantly. Early methods focused on phase difference distributions [12], while later studies incorporated nonlinear tools like recurrence plots and Lyapunov exponents to capture complex dynamics [2]. The Gait Synchronisation Index (GSI) has been used as a measure of coordination in diverse contexts, including virtual reality and treadmill experiments [7, 13]. Frequency domain techniques, such as wavelet analysis, can capture time-varying oscillatory patterns [14, 15].

Gait synchronisation is influenced by factors like leg length, sensory feedback, and cognitive load. Leg length impacts natural walking rhythms and energy efficiency, with mismatched lengths often increasing metabolic cost and reducing synchronisation [2, 16]. Therefore, the generally larger height disparity between females and males [17] may also affect synchronisation. Sensory feedback is another key factor, with visual cues and hand contact facilitating enhanced coordination and smoother gait synchronisation [3, 18]. Additionally, task complexity has been shown to affect synchronisation, with simpler tasks leading to stronger coordination [4].

3 Dataset

This study uses the DIAMOR dataset [19], a publicly available dataset capturing pedestrian movements within an underground street network in Osaka, Japan (see Fig. 1-a). Experimentation was reviewed and approved by ATR ethics board with document number 10-502-1 and the dataset consists of two primary components: pedestrian trajectories and video recordings.

The range data were recorded by laser sensors operating at 25 ms/scan. The publicly available trajectories were extracted from raw range readings [20] (see Fig. 1-b) at a rate of 20 to 50 Hz with a position accuracy of roughly 5 cm [19]. A Savitzky-Golay filter was applied on trajectories with a window size of 0.25 s and a polynomial order of 2, ensuring removal of measurement noise while preserving the oscillatory patterns associated with gait.

Table 1: Breakdown of the number of dyads for (a) different intensities of interaction.

Intensity of interaction	Count
Interaction 0	60
Interaction 1	83
Interaction 2	328
Interaction 3	45

The video data, which captured a portion of the underground network, were used to annotate trajectories with group membership and interaction levels. However, these recordings are not publicly available due to privacy considerations. A two-step annotation process was conducted: first, two coders identified group membership by observing walking patterns and demographics.

An inter-rater reliability analysis on group annotations indicated a strong agreement with a Cohen's $\kappa = 0.96$. Next, interaction intensity within dyads was annotated on a four-level scale (0: no interaction to 3: high interaction) by two other coders. They underwent a free viewing session for developing an understanding of the different interaction levels before the annotation process rather than relying on predefined criteria. The coders were found to have an acceptable level of agreement on interaction intensity with a Krippendorff's $\alpha = 0.67$. Note that at the end of this coding process, 516 dyads were labeled for intensity of interaction as demonstrated in Table 1. In addition to these dyads, our analysis involves a baseline set which is comprised of 1000 randomly paired pedestrians.

4 Methods

We consider a pedestrian's trajectory as a sequence of positions $\mathbf{p}(t_k)$ and velocities $\mathbf{v}(t_k)$ of the centre of mass of the pedestrian, sampled at times t_k, with $k \in [0, N-1]$ and N being the number of samples. The trajectory is defined as

$$T = \left[(\mathbf{p}(t_0), \mathbf{v}(t_0)), (\mathbf{p}(t_1), \mathbf{v}(t_1)), \ldots, (\mathbf{p}(t_{N-1}), \mathbf{v}(t_{N-1}))\right].$$

The velocities are derived from the positions using a simple forward Euler difference.

To extract the motion of a pedestrian's centre of mass caused by gait-induced oscillations, a smoothed trajectory $\tilde{T}$ is generated by applying another Savitzky–Golay filter to the original trajectory T. This filter uses a larger window size of 2 seconds and the same polynomial order of 2 to flatten the trajectory to a degree that eliminates gait-induced oscillations (see Fig. 2-a). The gait residual γ_k are then calculated as the signed distance between the original trajectory point $\mathbf{p}(t_k)$ and its projection onto the smoothed trajectory line segment connecting $\mathbf{p}\ (t_{k-1})$ and $\mathbf{p}\ (t_{k+1})$ (see Fig. 2-b).

The Hilbert phase $\phi(t_k)$ of the γ_k signal is computed via the Hilbert transform, which generates the analytic signal, from which the instantaneous phase can be extracted to gain insights into the signal's frequency content and temporal evolution.

We compute the relative phase $\Delta\phi_{ij}$ between the gait residuals of two pedestrians i and j as the difference between their Hilbert phases, i.e. $\Delta\phi_{ij} = \phi_i - \phi_j$.

To analyze this relative phase, we use directional statistics. The mean relative phase $\overline{\Delta\phi_{ij}}$ is calculated as the circular mean of the relative phase distribution, while the phase variance $\sigma_{\Delta\phi_{ij}}$ is computed as the circular standard deviation.

(a)

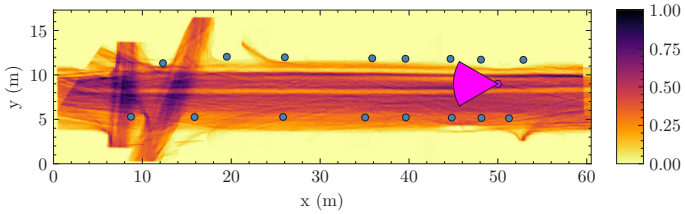

(b)

Figure 1: DIAMOR dataset. (a) Photograph of the underground pedestrian street network where the data were recorded, with sensors for pedestrian tracking marked in blue. (b) Normalised density map showing pedestrian distribution, created by dividing the area into 10 cm $\times$ 10 cm cells and normalizing counts by the maximum value. Darker areas represent higher densities. Blue dots mark the sensors, and the magenta wedge indicates the camera's field of view.

The Gait Synchronisation Index [7, 21] measures the gait synchronisation between two pedestrians using the Shannon entropy of their relative phase distribution. It is computed by binning the relative phase values and calculating the entropy

$$GSI_{ij} = 1 - \frac{H(\Delta\phi_{ij})}{\log_2(N_b)}, \tag{1}$$

where $H(\Delta\phi_{ij})$ is the entropy of the relative phase and N_b is the number of bins.

To provide a reference for synchronisation levels expected by chance, we also calculate the relative phase and GSI for baseline scenarios of randomly paired pedestrians.

5 Results and Discussion

Fig. 3 shows a polar histogram depicting the mean relative phase across varying interaction levels and a baseline condition. For the baseline scenario, the mean relative phase appears uniformly distributed around the circle, indicating no evident phase-locking behavior between pedestrians. This aligns with expectations for randomly paired pedestrians (B), who act independently and may only be synchronised by chance.

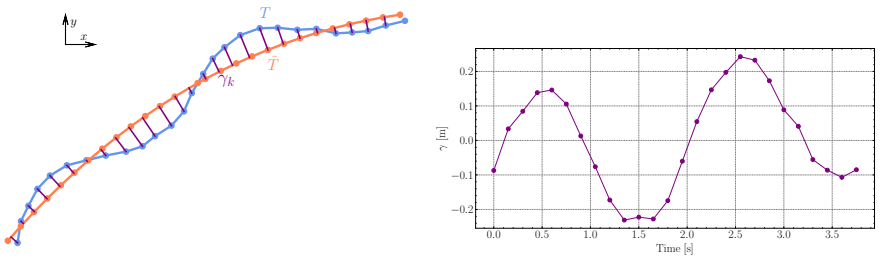

(a) (b)

Figure 2: Gait residual extraction. (a) Hypothetical (blue) and smoothed (orange) pedestrian trajectories, with gait residuals (γ) as the signed distance between them. (b) Gait residuals for the trajectory in (a).

In contrast, the relative phase distributions for the interaction levels display a marked phase-locking trend around 0 radians, signifying a propensity for in-phase gait synchronisation as interactions increase.

Tab. 2 summarises the circular mean and variance of the relative phase. The mean relative phase shifts closer to 0° as interaction levels rise, ranging from −13.30° for dyads without interaction to 3.20° for strongly interacting pairs. Additionally, the circular variance declines with increasing interaction, from 0.75 for non-interacting dyads to 0.35 for those strongly interacting. In the baseline condition, a variance of 0.95 suggests a near-uniform distribution, consistent with the polar histogram observations.

Fig. 4 presents the mean GSI values across interaction levels and the baseline condition, with corresponding values detailed in Tab. 3. A separation between low (0 and 1) and high (2 and 3) interaction levels is observed, with the former exhibiting lower GSI. A Kruskal-Wallis test confirms a significant effect of interaction level on GSI values ($p = 7.98 \times 10^{-4}$).

The baseline GSI value of 0.13 is consistently lower than or equal to the GSI values across all interaction levels, confirming that dyads often exhibit higher GSI values than random pairings. A Student's t-test confirms that the baseline GSI is significantly lower than the GSI for all dyads ($p < 10^{-4}$).

Zivotofsky et al. [4] previously demonstrated the influence of cognitive load on gait synchronisation, finding that simple dual tasks enhance gait synchronisation while complex ones reduce it. Our results suggest that social interactions play a similar role, acting as a form of small cognitive load that enhances gait synchronisation. Notably, this indicates that social interactions may not impose substantial cognitive demands, even at higher levels of intensity.

While no direct evidence exists in the literature regarding the effect of interpersonal distance on gait synchronisation, we examine this possibility by analyzing GSI values across varying distances between pedestrians.

Fig. 5-a shows the mean GSI values as a function of the distance between dyad members. A noticeable trend emerges where GSI values decline as interpersonal distance increases, indicating stronger gait synchronisation at closer proximities.

It is crucial to note that the distance between dyad members is not independent of their interaction level. In Fig. 5-b, the distribution of distances at various interaction levels reveals that higher interaction levels are associated with closer proximity. This relationship has been previously modeled in the literature [22, 23]. To disentangle the effects of distance and interaction on gait synchronisation, their independent contributions must be assessed.

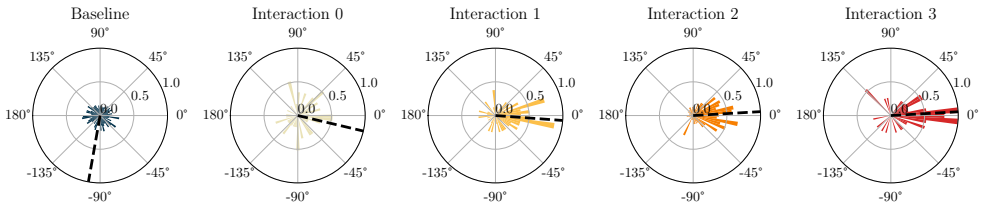

Figure 3: Polar histogram of the mean relative phase for different levels of interaction and baseline.

Table 2: Circular mean and variance of the relative phase between dyad members for different intensities of interaction and baseline pairs.

Intensity of interaction	Mean relative phase (°)	Variance
Baseline	−99.99	0.96
Interaction 0	−13.30	0.75
Interaction 1	−4.20	0.53
Interaction 2	3.31	0.47
Interaction 3	3.20	0.35

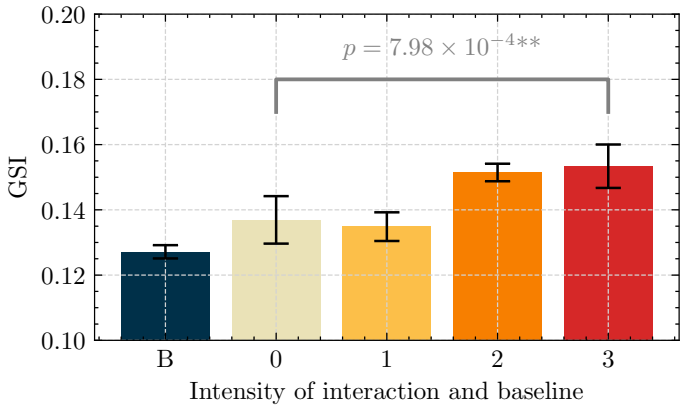

Figure 4: Mean GSI values for different levels of interaction and baseline.

Fig. 5-c presents GSI values binned by distance and separated by interaction levels. The negative correlation between distance and GSI persists across all interaction levels, with greater distances corresponding to lower GSI. It is harder to discern the effect of interaction level for given distances due to the reduced sample sizes which produce empty bins and higher variance in the data. Nonetheless, we observe that interaction level 3 tends to have higher GSI values than the other interaction levels (except for the [0.8, 1.1] m bin). Interaction level 2 is also consistently higher than interaction level 1. Non-interacting dyads (interaction level 0) exhibit the lowest GSI values among all interaction levels in the [1.1, 1.4] m bin, as well as the lowest observed GSI across all conditions in the largest distance bin ([1.7, 2.0] m).

Table 3: GSI for different intensities of interaction. Kruskal-Wallis p-values for the difference between the intensities of interaction and Student's t-test p-values for the difference between all dyads and the baseline are also shown.

Intensity of interaction	GSI	
Interaction 0	0.14 ± 0.06	$\mathbf{7.98 \times 10^{-4}}$
Interaction 1	0.13 ± 0.04	
Interaction 2	0.15 ± 0.05	
Interaction 3	0.15 ± 0.04	
All	0.15 ± 0.05	$\mathbf{< 10^{-4}}$
Baseline	0.13 ± 0.05	

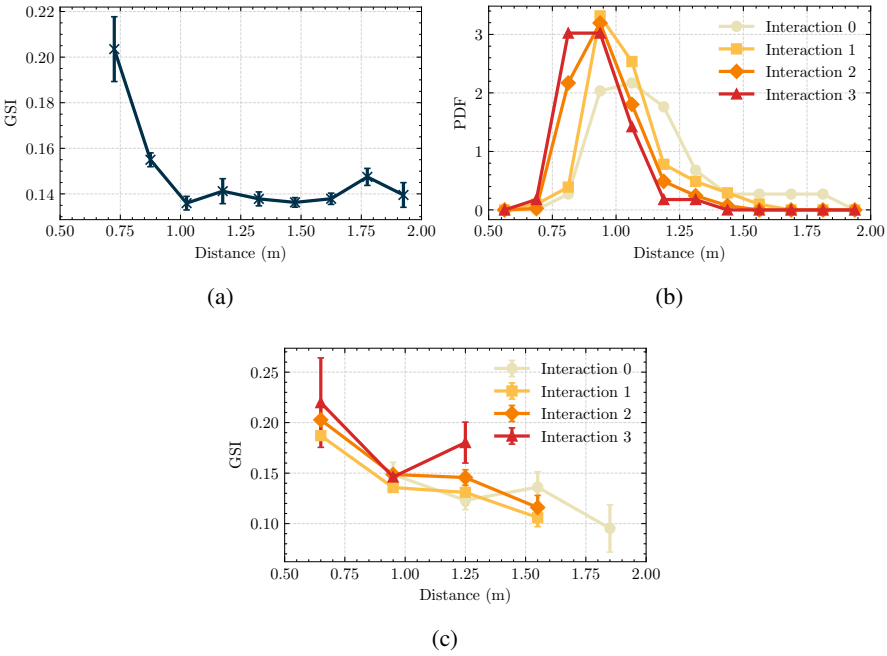

(a) (b)

(c)

Figure 5: (a) GSI as a function of interpersonal distance. (b) Distribution of interpersonal distances for different interaction levels. (c) GSI as a function of interpersonal distance for different interaction levels.

6 Limitations

The computation of GSI involves two hyperparameters, which affect the outcome significantly, namely length of time window and histogram bin size. Since the data are collected under ecological conditions, the observations have varying durations. To be able compare GSI values in an objective way, it was necessary to partition the relative phase sequences into equal length segments before applying Eq. 1. Testing several values, we chose to segment relative phase sequences into non-overlapping 5 second-long segments, which is comparable to the choice of [5]. We represent the level of synchronisation of a dyad or baseline pair with the mean GSI over all its segments. The second factor relates the computation of the

Shannon entropy of the relative phase distribution $H(\Delta\phi_{ij})$ in Eq. 1. This involves binning the relative phase values into N_b bins and generating a histogram from these values. Testing several values, we decided to use $N_b = 32$. Although the chosen length of time window and histogram bin size result in a reasonable compromise, GSI has seen to be very sensitive to these hyperparameters. In the future, it is considered to merge GSI or replace it with time domain methods such as recurrence analysis or time-frequency domain methods such as wavelet coherence, which do not entail these issues.

Furthermore, interpersonal distance and interaction level are not independent variables [23]. So for future work it will be important to understand whether higher synchronisation is due only to be closer in space or there is also a distinctive effect of interaction intensity.

7 Conclusion

This study investigates spontaneous gait synchronisation in social groups within a natural environment, using a pedestrian trajectory dataset collected in a public space. By analyzing gait residuals and relative phase differences, we quantify synchronisation and explore the influence of social interactions and interpersonal distances on gait synchronisation.

Our results demonstrate that dyads with higher interaction levels exhibit more phase locking around zero, lower phase variance, and higher synchronisation (measured by the GSI) compared to less interactive dyads and baseline pairs. These findings suggest that social interactions significantly influence gait synchronisation. While previous studies on cognitive load [4] have shown that simple tasks enhance synchronisation and complex tasks reduce it, our results indicate that social interactions act as a form of small cognitive load that enhances synchronisation, even at higher levels of intensity.

Additionally, we observe a negative correlation between interpersonal distance and gait synchronisation, with closer proximities fostering stronger synchronisation. However, this relationship is intertwined with interaction levels, as pedestrians with higher interaction levels tend to maintain closer distances.

While these findings provide valuable insights into pedestrian dynamics, several limitations should be acknowledged. When analyzing data by distance and separating levels of interaction, the resulting sample sizes became relatively small, which may affect the reliability of observed patterns. Future work should leverage larger datasets to provide stronger statistical power and validate these findings. Additionally, future studies may use alternative metrics for gait synchronisation, such as Wavelet Phase Coherence or Recurrence Quantification Analysis, to ensure robustness and reliability.

Understanding how pedestrians synchronise their gaits has practical implications in various fields, including structural design, rehabilitation or robotics. Insights into gait synchronisation can inform the design of pedestrian bridges and other structures to prevent resonance effects caused by synchronised walking, which can compromise structural integrity [24]. In rehabilitation, gait synchronisation can be used as a therapeutic tool to improve motor coordination and balance in patients with gait disorders. Since interaction levels influence gait synchronisation, rehabilitation programs could incorporate social interactions to enhance coordination and recovery [25]. In robotics, understanding gait synchronisation can improve the design of socially-aware robots that interact with humans in public spaces. By mimicking human gait synchronisation behaviors, robots can navigate crowded environments more naturally, enhancing their social acceptance and safety [26].

References

[1] D.T. Felsberg, C.K. Rhea, Arch. Rehabil. Res. Clin. Transl. **3**, 100097 (2020)
[2] J.A. Nessler, S. Gilliland, Hum. Mov. Sci. **28**, 772 (2009)
[3] F. Sylos-Labini, A. d'Avella, F. Lacquaniti, Y. Ivanenko, Front. Physiol. **9** (2018)
[4] A.Z. Zivotofsky, H. Bernad-Elazari, P. Grossman, J.M. Hausdorff, Hum. Mov. Sci. **59**, 20 (2018)
[5] C. Chambers, G. Kong, K. Wei, K. Kording, PLoS ONE **14**, e0217861 (2019)
[6] A. Hajnal, F.H. Durgin, Experimental brain research **241**, 469 (2023)
[7] A.Z. Zivotofsky, L. Gruendlinger, J.M. Hausdorff, Hum. Mov. Sci. **31**, 1268 (2012)
[8] A. Gregorj, Z. Yücel, F. Zanlungo, C. Feliciani, T. Kanda, Scientific reports **13**, 5756 (2023)
[9] M. Biswas, M. Brass, Plos one **19**, e0308843 (2024)
[10] G. Atherton, L. Cross, Psychological Studies **65**, 351 (2020)
[11] L. Cross, M. Turgeon, G. Atherton, Current Psychology **40**, 3393 (2021)
[12] L.K. Miles, J.L. Griffiths, M.J. Richardson, C.N. Macrae, Eur. J. Soc. Psychol. **40**, 52 (2010)
[13] A.A. Soczawa-Stronczyk, M. Bocian, R. Soc. Open Sci. **7**, 200622 (2020)
[14] J. Issartel, L. Marin, P. Gaillot, T. Bardainne, M. Cadopi, J. Mot. Behav. **38**, 139 (2006)
[15] A. Grinsted, J.C. Moore, S. Jevrejeva, Nonlinear Process. Geophys. **11**, 561 (2004)
[16] M.Y. Zarrugh, F.N. Todd, H.J. Ralston, Eur. J. Appl. Physiol. Occup. Physiol. **33**, 293 (1975)
[17] Z. Yücel, F. Zanlungo, T. Kanda, *Gender Profiling of Pedestrian Dyads*, in *Traffic and Granular Flow 2019*, edited by I. Zuriguel, A. Garcimartin, R. Cruz (Springer International Publishing, Cham, 2020), pp. 299–305
[18] S.J. Harrison, M.J. Richardson, J. Mot. Behav. **41**, 519 (2009)
[19] T. Kanda, D. Brščić, *Data set: Pedestrian tracking with group annotations* (2015), `https://dil.atr.jp/ISL/sets/groups/`
[20] D.F. Glas, T. Miyashita, H. Ishiguro, N. Hagita, Advanced robotics **23**, 405 (2009)
[21] P. Tass, M.G. Rosenblum, J. Weule, J. Kurths, A. Pikovsky, J. Volkmann, A. Schnitzler, H.J. Freund, Phys. Rev. Lett. **81**, 3291 (1998)
[22] F. Zanlungo, T. Ikeda, T. Kanda, Phys. Rev. E. **89**, 012811 (2014)
[23] Z. Yücel, F. Zanlungo, M. Shiomi, Adv. Robot. **32**, 137 (2018)
[24] M. Bocian, J. Brownjohn, V. Racic, D. Hester, A. Quattrone, L. Gilbert, R. Beasley, Mech. Syst. Signal Process. **105**, 502 (2018)
[25] H. Uchitomi, K.i. Ogawa, S. Orimo, Y. Wada, Y. Miyake, PLoS ONE **11**, e0155540 (2016)
[26] Y. Morales, T. Kanda, N. Hagita, ACM Trans. Hum.-Robot Interact. **3**, 50–73 (2014)